# Supplementary Materials for

## LncRNA Uc003xsl.1-mediated activation of the NF-κB/IL8 axis promotes progression of triple-negative breast cancer

Ying Xu[#], Wei Ren[#], Qingjian Li[#], Chaohui Duan[#], Xiaorong Lin, Zhuofei Bi, Kaiyun You,

Qian Hu, Ning Xie, Yunfang Yu, Xiaoding Xu[*], Hai Hu[*], Herui Yao[*]

*Corresponding authors: xuxiaod5@mail.sysu.edu.cn; huhai@mail.sysu.edu.cn;

yaoherui@mail.sysu.edu.cn

**This PDF file includes:**

Supplementary Materials and Methods

Figures S1 to S9

**Supplementary Materials and Methods**

**Sequence of primers for real-time PCR**

Primers were synthesized by the IGE Biotechnology, China. The sequences of involved primers were as following:

NKRF: Forward 5'-CGGAGCGGGCGTAGTTTCTGA-3';

Reverse 5'-TCTGGTGAGGGCATACGGGAGC-3';

Uc003xsl.1: Forward 5'- ACAGCTCTGCCACTTTGTGA -3';

Reverse 5'- AGCAACACACCACAGCTTGA -3';

IL8 promotor: Forward 5'- GTGATGACTCAGGTTTGCCCTG -3';

Reverse 5'- GAGTGCTCCGGTGGCTTTTTA -3';

IL6: Forward 5'- AAGCCAGAGCTGTGCAGATGAGTA -3';

Reverse 5'- TGTCCTGCAGCCACTGGTTC -3';

IL1β: Forward 5'- AAGCCCTTGCTGTAGTGGTG -3';

Reverse 5'- GAAGCTGATGGCCCTAAACA -3';

IL8: Forward 5'-GCTCTCTTGGCAGCCTTCCTG-3';

Reverse 5'-GTCCAGACAGAGCTCTCTTCCATC-3'.

Trop2: Forward 5'- GACAACTGCACGTGTCCCAC -3';

Reverse 5'- AGAGGCCATCGTTGTCCACG -3';

β-actin: Forward 5'- TCATGAAGTGTGACGTGGACATC -3';

Reverse 5'- CAGGAGGAGCAATGATCTTGATCT -3';


**Plasmids and si-RNAs**

The expression plasmids for Uc003xsl.1, antisense, and fragments of Uc003xsl.1 and expression plasmids for NKRF or Flag-tagged NKRF fragments (pcDNA3.1-NKRF1, pcDNA3.1-NKRF2, pcDNA3.1-NKRF3, pcDNA3.1-NKRF3-1, pcDNA3.1-NKRF3-2, pcDNA3.1-NKRF3-3, pcDNA3.1-NKRF3-3-del) were synthesized by the IGE Biotechnology, China. The pGL4.17 [luc2] vector was purchased from Promega, USA. The IL-8 promoter-driven luciferase reporter plasmid pGL4.17-IL8pr (nucleotides 1353–1482 of the *IL-8* gene) has been described(1). Site-directed mutagenesis of NRE and NF-κB sites was performed using the oligo-nucleotides described in Fig. 6. All mutations described above were introduced using the Quick ChangeTM site-directed mutagenesis kit (Stratagene, USA). Primer sequences used for polymerase chain reaction are available upon request. Sequences were confirmed by automated DNA sequencing on an Illumina HiSeq sequencer (Illumina, USA).

The si-RNAs were synthesized by the Gene Pharma, China. The sequences of involved si-RNAs were as following:

scramble-control siRNA: 5'-GGUAAUAGAGTAUATGGUAGG-3'

si-NC: 5'-UUGGUGUCCUAUUACUGGGTT-3';

si-Uc003xsl.1-1: 5'-AUCUCCCAGCUGUACUUUCTT-3';

si-Uc003xsl.1-2: 5'-AUGUGAGAGAUGAAGAUGGTT-3';

si-NKRF1: 5'-UAACUUCACAAGCAUAGCCTT-3';

si-NKRF2: 5'-ACAACUCUAACUUCAAUACTT-3';

si-IL8-1: 5'-UGAAUUCUCAGCCCUCUUCTT-3';

si-IL8-2: 5'-UCCUUGGCAAAACUGCACCTT-3';

si-P65-1: 5'-AUGACGUAAAGGGAUAGGGTT-3';

si-P65-2: 5'-UGGAGGAGAAGUCUUCAUCTT-3'.

**Cell cultures and primary cell isolation**

MDA-MB-231, BT- 549, MCF-7, T47D, BT-474 and SKBR3 breast cancer cell lines and MCF-10A breast epithelial lines were obtained from American Type Culture Collection (ATCC) and cultured according to the recommended protocols. The cells were tested every 3 months for *Mycoplasma* by means of the Mycoplasma Detection Kit (Solarbio, China), cultured for no more than 3 weeks and used for no longer than 10 passages.

For siRNA and stable plasmid DNA transfection, cells were transfected with specific siRNA duplexes targeting Uc003xsl.1, NKRF, P65 or IL8, or pcDNA3.1 vector expressing Uc003xsl.1, IL8 or NKRF construct using Lipofectamine 2000 (Invitrogen, USA) according to the manufacturer's instruction. To induce NF-κB activity, cells were treated with 20 ng/mL human TNF-α (Peprotech, USA) for 12 h.

For MDA-MB-231-P3 establishments, we firstly established an in vivo model by injecting MDA-MB-231cells into the tail veins of mice. As the breast tumor cells successfully grew into metastatic lung tumors, freshly isolated tumor tissues from the mice lungs were mechanically dissociated, treated with collagenase (Gibco, USA) at 37°C for 2 h, filtered, and washed twice. The homogenate suspension of tumors cells was then cultured and amplified in vitro, followed by re-injected into the tail veins of mice for lung metastasis. After three rounds of selection, a highly metastatic subline, MDA-MB-231-P3, was established.

**In situ hybridization and data analysis**

Formalin-fixed, paraffin-embedded sections of TNBC tissues and normal adjacent tissues were obtained from the Breast Tumor Center at Sun Yat-Sen Memorial Hospital. Following wax removal and rehydration, the samples were digested with Proteinase K, hybridized with lncRNA Uc003xsl.1 specific probe (Advanced Cell Diagnostics, USA) at 40°C for 2h. Subsequently, the preamplifier was hybridized to the target probes at 40°C and amplified with six cycles of hybridization, followed by two washes. The avidin-biotin-peroxidase detection systems with the DAB substrate were used to mark the location of the antigen. Then, the nuclei were counterstained with hematoxylin. Finally, slides are dehydrated with 100% ethanol and xylene, and mounted in a xylene-based mounting media. The Uc003xsl.1 expression in TNBC tissues and normal adjacent tissues was evaluated by using the histochemical score (H-score). The intensity of staining was multiplied by the percentage of positive cells, and the H-score (0–300) of each tissue was obtained for statistical analysis. The staining H-score of 110 was used as a cutoff value based on the frequency of the H-scores for Uc003xsl.1 expression. The expression levels of Uc003xsl.1 were defined as high (Uc003xsl.1-high) or low (Uc003xsl.1-low). Staining was reviewed and scored by two experienced independent pathologists.

**MTS, EdU assays, and Transwell assay**

Cell proliferation was measured with MTT and EdU assays, following the instructions. Cells were transfected with siRNA or overexpression plasmid, followed by seeding in 96-well plates at a density of $4 \times 10^3$ cells per well, and cultured overnight. For MTS assays, Cells were treated with MTS solution according to the manufacturer's instructions from the MTS kit (APExBIO, USA). The number of viable cells was measured by OD490 with a microplate reader (Epoch,

BioTek, USA) every 24 h for 5 days. For EdU assays, 100μL of EdU was added to the cells according to the manufacturer's instructions from the EdU kit (RIB&BIO, China). The images were obtained with an Olympus laser scanning microscope system.

For Transwell assays, $5 \times 10^5$ cells were plated in 12-well plates (Corning Costar Corp, USA). For migration assays, cells were placed in the upper chambers of non-coated membranes. For invasion assays, the membranes of upper chambers were 1:8 diluted and Matrigel-coated (BD Biosciences, USA). All lower chambers were filled with 800 μL of medium containing 30% FBS. After 24 or 48 h incubation at 37 °C, the number of cells that migrated or invaded was fixed and stained with crystal violet, then was imaged and counted in three fields under a 100 × objective lens using a microscope.

**Rapid amplification of cDNA ends (RACE)**

The 5' and 3' RACE assays were performed following the instructions of a SMARTer RACE kit (CLONTECH Laboratories, USA). The RACE PCR products were separated on a 1% agarose gel and further subjected to bidirectional sequencing. Uc003xsl.1-specific nested PCR primers sequences were used for 5' and 3' RACE analysis. The sequence data are deposited in GenBank (MW417110).

**Nuclear-plasma fractionation assays**

Adherent cells were collected with trypsin-EDTA and suspended with PBS. The nuclear and cytosolic fractionation of cells were separated using the NE-PER™ Nuclear and Cytoplasmic Extraction Reagents (Thermo Scientific, USA) following the manufacturer′s instructions.

Briefly, for plasma fractionation, 1 x 10$^7$ cells were harvested and washed with PBS. Then ice-cold CER I and CER II were added and incubated for 10 min on ice. Cells were centrifuged for 5 min at 12,000 x g and the supernatant was kept. Then suspended the pellet in ice-cold NER and vortexed for 15 seconds every 10 minutes, for a total of 40 minutes. After centrifuging the tube at 12,000 x g for 10 minutes, we collected the supernatant as nuclear fractionation. The plasma portion and nuclear extract fraction were kept at -80°C until use.

**Western blotting**

fter separation in 10% SDS–PAGE gel, protein extracts were transferred onto a poly-vinylidene fluoride (PVDF) membrane and placed into 5% BSA for blocking at room temperature for 1h. Subsequently, primary antibodies were added and incubated with anti-NKRF (ab168829, 1:1000, Abcam, USA), anti-P65 (8244, 1:1000, Cell Signaling Technology, USA), anti-pP65 (3039, 1:1000, Cell Signaling Technology, USA), Trop2 antibody (47866, 1:1000, Cell Signaling Technology, USA) and GAPDH antibody (8884, 1: 5000, Cell Signaling Technology, USA) overnight at 4°C. Finally, the blots were incubated with secondary antibodies (anti- rabbit IgG HRP-linked antibody, 1:1000, Cell Signaling Technology, USA). The proteins were visualized with a Tanon-5200 Chemiluminescent Imaging System (Tanon, China).

**Mass spectrometry analysis**

To identify specific Uc003xsl.1 interactors, Uc003xsl.1 and Antisense Uc003xsl.1 pull-down eluates were compared. The band that was pre-dominantly represented in the Uc003xsl.1 pulldown sample were chosen. The band was then excised to perform mass spectrometry

analysis as previously described(2). Briefly, the Q Exactive mass spectrometer (Thermo Fisher Scientific, USA) was used. Peptide identification was carried out on the Mascot software (Version 2.3.01, Matrix Science, UK) using the UniProt database search algorithm and the integrated false discovery rate (FDR) analysis function. The data were searched against a protein sequence database downloaded from 2019_uni_human human (172,061 sequences, 53,783,369 residues). The MS/MS spectra were searched against a decoy database to estimate the false discovery rate FDR (<0.05) for peptide identification.

**Dual-luciferase reporter assays**

The indicated regions of NF-κB and IL8 promoter were directly inserted into pGL4.10 luciferase reporter plasmid. The pcDNA3.1-NKRF, pcDNA3.1-NKRF3-D1, pcDNA3.1-NKRF3-D2, pcDNA3.1-NKRF3-D3 and pcDNA3.1-NKRF-DR3H were co-transfected into MDA-MB-231-P3 cells. The pGL4.10 (luc2) vector was utilized as a negative control. The luciferase activities were detected using the Dual-Luciferase Reporter Assay System (Promega, USA). Renilla luciferase activity was normalized against Firefly luciferase activity for intra-experimental transfection efficiency.

**Immunofluorescence**

Cells were fixed using 4% paraformaldehyde after being seeded in a culture dish and incubated for 24h. Cells were incubated with 0.1% Triton 100X in PBS for 15min to be permeated. After being blocked with 10% goat serum for 1 h, cells were incubated with primary Trop2 antibody (Sigma, USA, 1:100) at 4 °C overnight. PBS was added to wash the cells and then cells were

incubated with secondary fluorescent antibody for 1 hour at room temperature before imaging.

**Immunohistochemistry (IHC)**

Immunohistochemical staining was conducted on formalin-fixed paraffin-embedded tissue sections using a Kit (Zhongshan Golden Bridge, China) in accordance to the manufacturer's protocol. Briefly, deparaffinized tissue sections were heated to retrieve antigen, treated with 3% $H_2O_2$ to quench endogenous peroxidase activity followed by being blocked with goat serum and incubated using primary antibody targeting Trop2 (Sigma, USA, 1:800) at 4 °C overnight. Subsequently, sections were incubated with horseradish peroxidase-conjugated goat anti-rabbit IgG for 30 min at 37 °C and then developed with daiminobenezidine (DAB). The evaluation of Trop2 expression was quantified independently by two observers. The IHC Trop2 score was evaluated according to the percentage of positive cells and staining intensity. We graded the staining intensity on a scale of 0 to 3: 0, negative; 1, weak (light yellow); 2, moderate (yellow–brown); 3, strong (brown). We calculated the percentage of cells at each staining intensity level so that we can derive the final Trop2 score with the formula: [1 × (% cells 1+) + 2 × (% cells 2+) + 3 × (% cells 3+)].

**RNA-seq analysis**

Total RNA was extracted from breast cancer fresh tissues, including 3 TNBC tissues, 3 luminal breast cancer tissues, normal MDA-MB-231 cells, and highly metastatic MDA-MB-231-P3 cells. The quality of the RNA was assessed with the Agilent Bioanalyzer 2100. Transcriptome libraries from the mRNA fractions were generated following the RNA-Seq protocol (Illumina,

USA). Each sample was sequenced in a single lane with the Illumina PE150 Analyzer (Illumina, USA) on a 150-bp paired-end run.

For strand-specific library construction, dUTP method of second-strand marking was employed as described(3). For the data processing, the raw sequencing reads were aligned to the human reference genome (hg19) using the splice-aware aligner HISAT2. Read counts for each gene were normalized into FPKM (Fragments Per Kilobase of transcript per Million mapped reads) values. The cutoff of differential gene expression was FDR <0.05, normalized by the respective control group. The differential expressed gene profiles in TNBC tissues and luminal breast cancer tissues were presented in Supplementary Table S1, and MAD-MB-231 and highly metastatic MDA-MB-231-P3 cells were displayed in Supplementary Table S2. Expression profile data are deposited in GEO (GSE163953).

**Generation of TACSTD2/ Trop2-knockout cell lines with the CRISPR/Cas9 system**

The backbone plasmids Lenti-sgRNA-EF1a and Lenti-CAS9-puro were obtained from GeneChem CO., Ltd (Shanghai, China). To construct the double nicking Trop2-sgRNA-guided CRISPR/Cas9 plasmids, a pair of oligos (sgRNA1: GCACCAGCTCATCGCAGCGT and sgRNA2: CGCACCAGCACACCGACGTC) were designed and subcloned into a Cas9 backbone. Cells were first infected with lenti-cas9 and then selected using puromycin. The stable sub-lines were then infected with lenti-sgRNA to specifically knock out the target genes. The KO efficiency of MDA-MB-231-P3 cells were detected by q-PCR and Western blotting after the infection of Trop2-sgRNA-guided CRISPR/Cas9 plasmids for 7 days.

**Preparation of nanoparticles (NPs)**

PDSA (poly disulfide amide), polymers were dissolved in N, N'-dimethylformamide (DMF) to form a homogenous solution with a concentration of 10 mg/mL. Next, 200 µL of PDSA polymer solution, 140 µL of DSPE-PEG5k solution (20 mg/mL in DMF), and 20 µL DSPE-PEG-NHS (20 mg/mL in DMF) were prepared and mixed with a compound of 1 nmol si-Uc003xsl.1 (0.1 nmol/µL aqueous solution), 50 µL of G0-C14 (5 mg/mL in DMF) for si-Uc003xsl.1 NPs, and 50 µL of Trop2 antibodies (Sigma, USA) for si- Uc003xsl.1/Trop2 NPs. Then we added drops of the mixture to five mL of deionized water and vigorously stirred it (1400 rpm). Organic solvent and free compounds were removed by transferring the NP dispersion to an ultrafiltration device (EMD Millipore, MWCO 100 K) and centrifuging. Finally, the aimed NPs were dispersed in 1mL of PBS buffer (pH 7.4).

**Characterizations of NPs**

Size and zeta potential were determined by dynamic light scattering (DLS, Brookhaven Instruments Corporation). NP morphology was visualized with a transmission electron microscope (TEM, Tecnai G2 Spirit BioTWIN). Samples were stained with 1% uranyl acetate and air-dried before observation. The cellular uptake of si-Uc003xsl.1 and si-Uc003xsl.1/Trop2 loaded NPs was measured by flow cytometry. MDA-MB-231-P3 cells were incubated with the Cy5-naked siRNA, Cy5-si-Uc003xsl.1 NPs, and Cy5-si-Uc003xsl.1/Trop2 NPs at 37 °C for 4 h at a 1 nM siRNA dose. Then the mean fluorescence intensity (MFI) were measured by a microplate reader (BioTek Instruments, USA).

**Pharmacokinetics study**

Healthy female BALB/c mice were randomly divided into three groups (n = 3) and given an intravenous injection of either (i) naked Cy5-si-Uc003xsl.1, (ii) Cy5-si-Uc003xsl.1 NPs, or (iii) Cy5-si-Uc003xsl.1/Trop2 NPs at a 1 nmol siRNA dose in 200 μL of PBS buffer per mouse. Then 20 μL of orbital vein blood was collected at different time points, followed by evaluating the fluorescence intensity of cy5-labelled siRNA in the blood with a microplate reader (BioTek Instruments, USA).

**Bio-distribution**

The non-tumor bearing, MDA-MB-231-P3 tumor-bearing or Trop2-KO tumor-bearing female athymic nude mice were randomly divided into three groups (n = 3) and given an intravenous injection of either (i) naked Cy5-si-Uc003xsl.1, (ii) Cy5-si-Uc003xsl.1 NPs, or (iii) Cy5-si-Uc003xsl.1/Trop2 NPs at a 1 nmol siRNA dose in 200 μL of PBS buffer per mouse. The harvested tumors and main organs of the mice were imaged with the Maestro 2 In-Vivo Imaging System (CRi Inc, USA) 24 h after the injection. Then NP accumulation was verified by quantifying the accumulation of NPs in tumors and organs. The tissues and organs were homogenated and the fluorescence intensity of Cy5-siUc003xsl.1 was examined by microplate reader.

**Tumor xenografts**

Female nude mice (4–6-weeks-old) were bred and maintained under SPF barrier facilities at the Animal Experiment Center of Sun Yat-sen University. All procedures were approved by the

Institutional Animal Care and Use Committee (IACUC) of Sun Yat-sen University and conformed to the legal mandates and national guidelines for the care and maintenance of laboratory animals. MDA-MB-231-P3 cells stably transfected with two Uc003xsl.1-shRNAs or sh-NC were re-suspended at $1 \times 10^7$ cells/mL. For the subcutaneous tumorigenicity model, a total of 100 μL of suspended cells were injected subcutaneously into the left armpit of nude mice. Tumor growth was evaluated by monitoring tumor volume (TV = 1⁄2 length x width$^2$) every 5 days for 1 month. When the xenografts became palpable (xenograft volume reached 200 mm$^3$) the mice were killed, and their tumor xenografts, lungs, and livers were harvested for further evaluation. For the metastatic lung model, a total of $1 \times 10^6$ cells of MDA-MB-231-P3-luciferase cells stably-transfected with sh-Uc003xsl.1 or control vector were injected into tail veins of BALB/c nude mice. The process of lung metastasis was detected by an in vivo imaging system for 7 weeks. Animals were sacrificed by cervical dislocation at 7 weeks post-injection. Lungs were harvested for further evaluation.

For the nanodrug experiments, MDA-MB-231-P3 or MDA-MB-231-P3-Trop2-KO tumor-bearing female nude mice were randomly divided into four groups. After the xenograft volume reached 200mm$^3$ (the xenograft tumor model) or the lung metastasis (the metastatic lung model) assessed by bioluminescent imaging, the mouse was intravenously injected with (i) PBS, (ii) scramble-control siRNA NPs, (iii) si-Uc003xsl.1 NPs, or (iv) si-Uc003xsl.1/Trop2 NPs at a 1 nmol siRNA dose per mouse once every two days. All the mice were administered by three consecutive injections injected with indicated dose through the tail vein. For the treatment of the xenograft tumor model, the animals were killed after 30 days of the last injections. For the treatment of the metastatic lung model, the animals were sacrificed after 21 days of the last

injection. Tumors and harvested organs were subjected to hematoxylin-eosin (H&E) and further

IHC and ISH staining.

**References**

1. Nourbakhsh M, Kalble S, Dorrie A, Hauser H, Resch K, Kracht M. The NF-kappa b repressing factor is involved in basal repression and interleukin (IL)-1-induced activation of IL-8 transcription by binding to a conserved NF-kappa b-flanking sequence element. J Biol Chem **2001**;276:4501-8

2. Tsai MC, Manor O, Wan Y, Mosammaparast N, Wang JK, Lan F*, et al.* Long noncoding RNA as modular scaffold of histone modification complexes. Science (New York, NY) **2010**;329:689-93

3. Levin JZ, Yassour M, Adiconis X, Nusbaum C, Thompson DA, Friedman N*, et al.* Comprehensive comparative analysis of strand-specific RNA sequencing methods. Nat Methods **2010**;7:709-15

# Supplementary Figure S1

A



B

Lung



C

Cohort 2



D

Cohort 2



E

Cohort 2
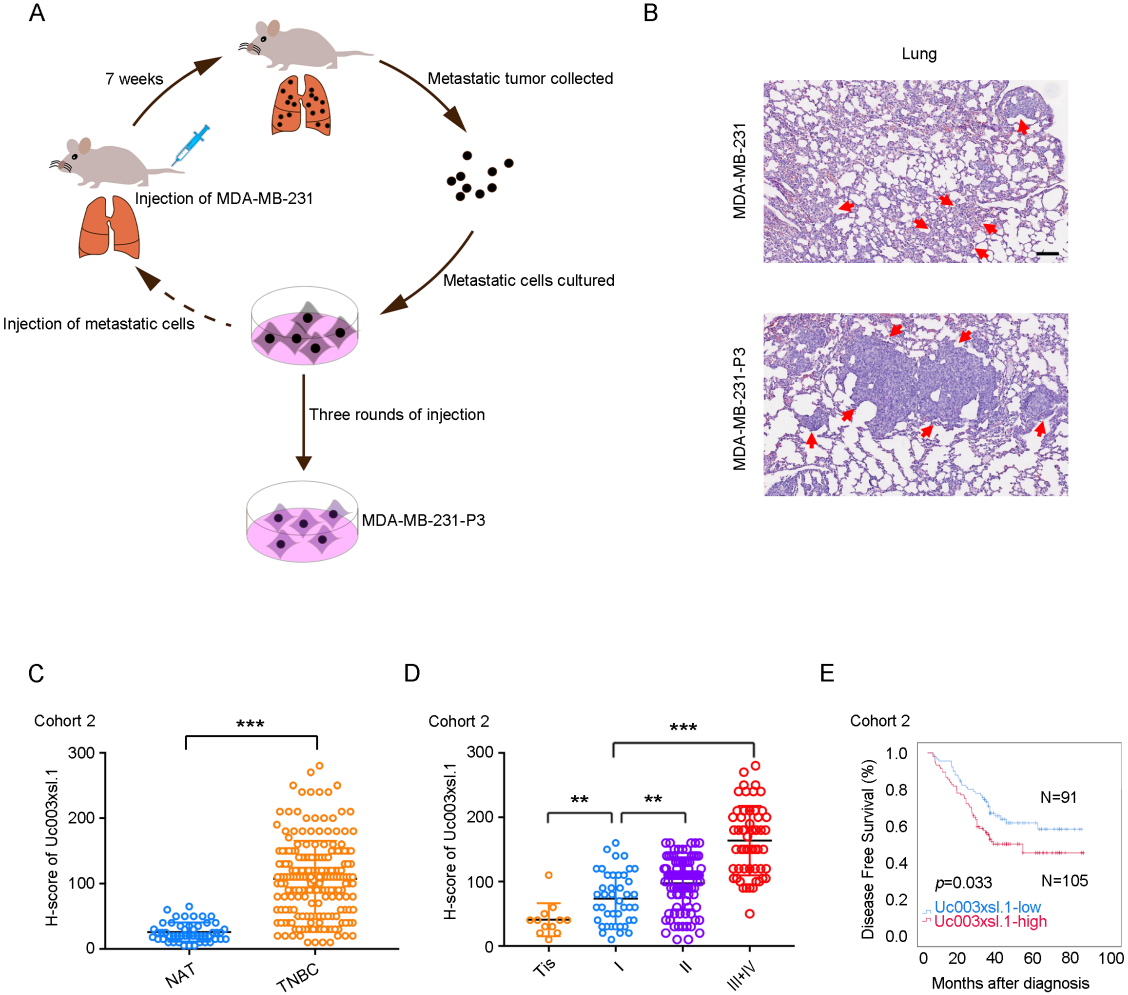


Supplementary Fig. S1

**Supplementary Figure S1. Clinical relevance of candidate lncRNA Uc003xsl.1 in TNBC.**

(A) Schematic illustration of a highly metastatic subline, MDA-MB-231-P3, was established.

(B) Lung section was stained by H&E from MDA-MB-231 groups and MDA-MB-231-P3

groups. (C) ISH analysis of Uc003xsl.1 expression in the paraffin-embedded NAT (n = 60) and

tumor sections of TNBCs (n = 196) (cohort 2). (D) Uc003xsl.1 expression was significantly
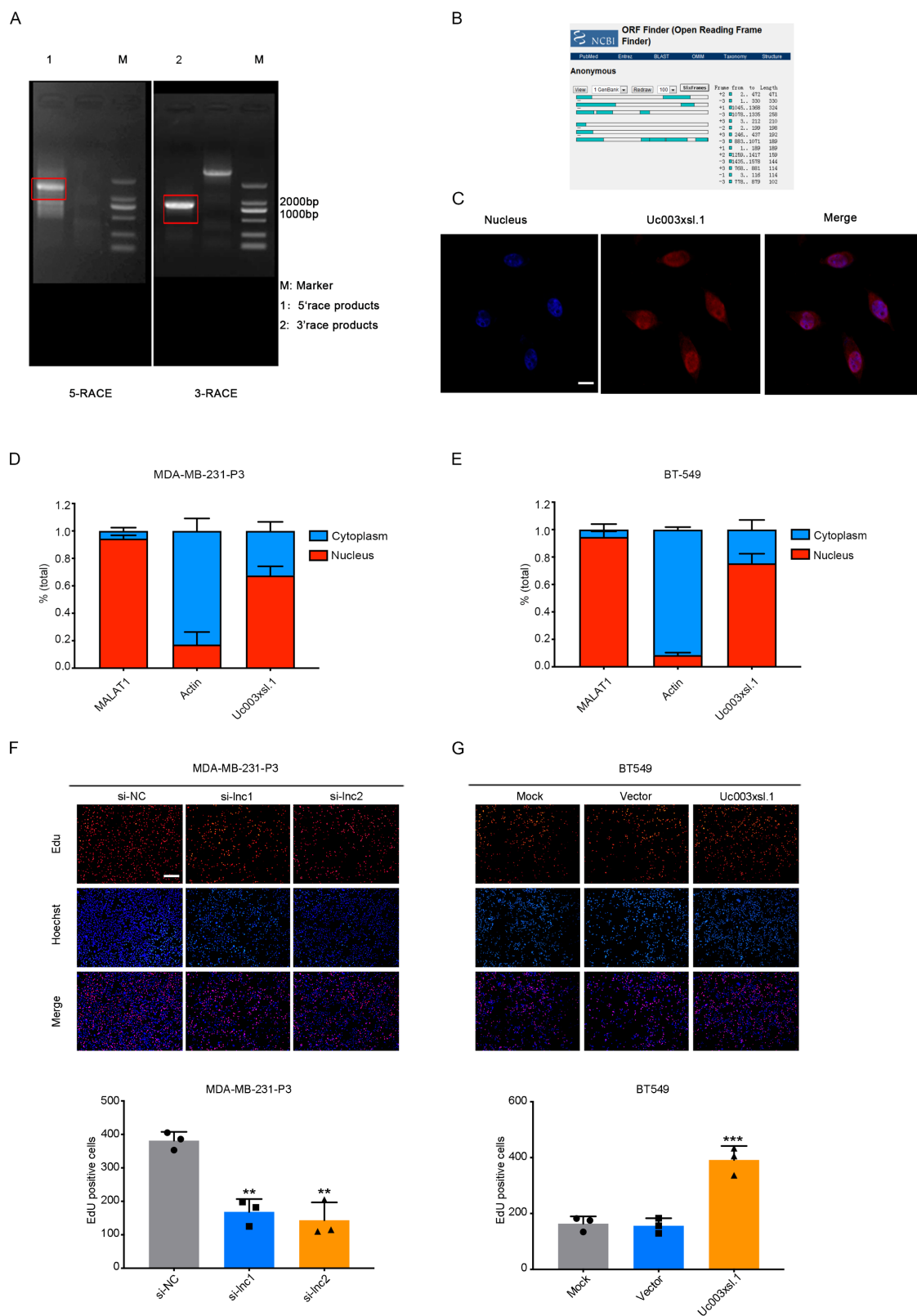
higher in patients with advanced TNM stage. (E) Patients with high levels of Uc003xsl.1

showed reduced DFS compared to patients with low levels of Uc003xsl.1. Error bars represent

standard deviations of three independent experiments. $**p < 0.01$, $***p < 0.001$.
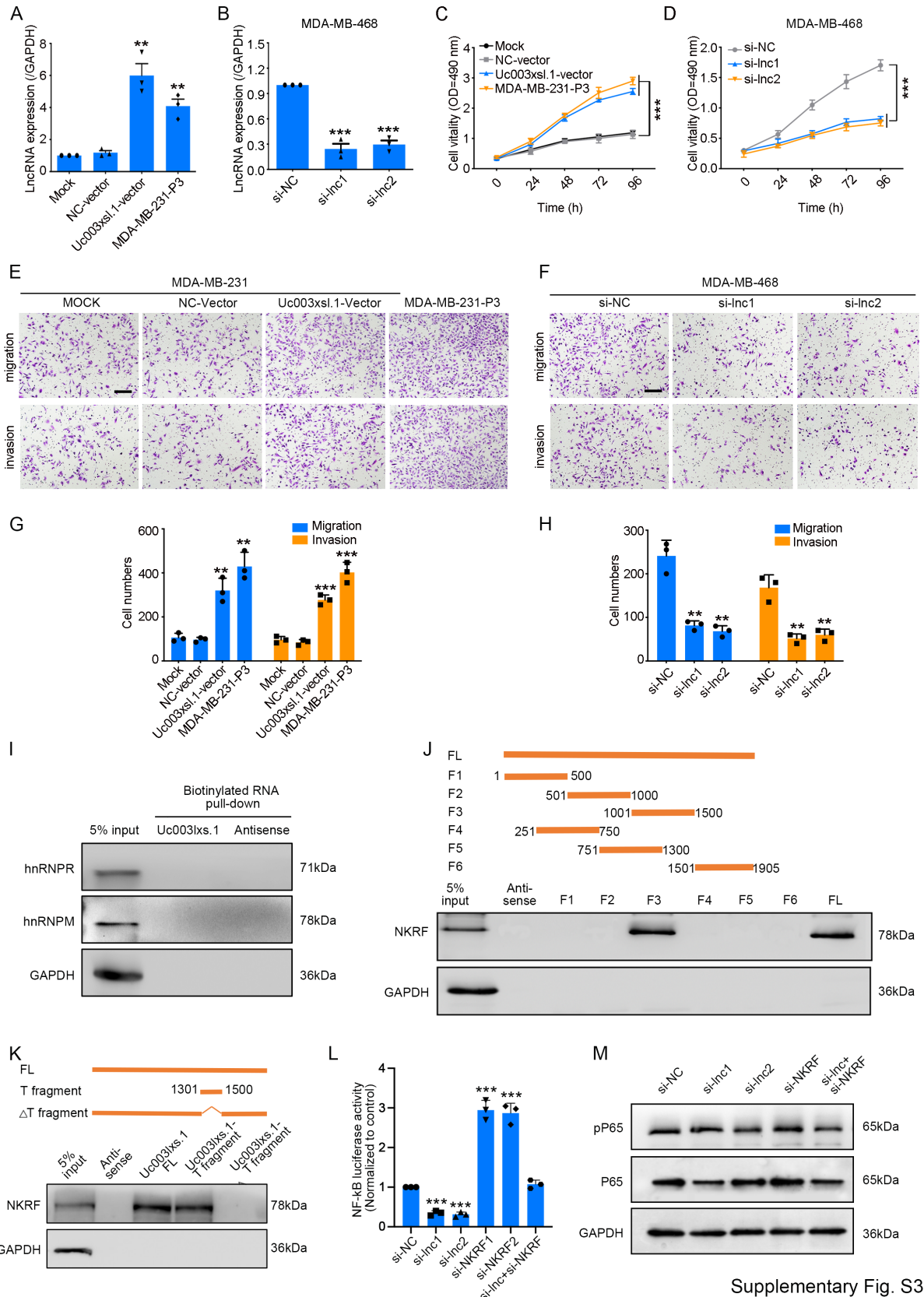
# Supplementary Figure S2

**Supplementary Figure S2. Uc003xsl.1 acts as an oncogenic lncRNA in TNBC.**

(A) 5'and 3' RACE assay was performed to measure the full-length sequence of Uc003xsl.1. Representative images display the 5' RACE and 3' RACE products separated by 1% agarose gel electrophoresis. (B) ORF Finder from the National Center for Biotechnology Information showed that Uc003xsl.1 sequences did not contain any ORF for potential protein-encoding segments. (C) Uc003xsl.1 localization was assessed by FISH in MDA-MB-231-P3 cells. (D-E) Uc003xsl.1 expression in the cytoplasm and nucleus of MDA-MB-231-P3 cells (D) and BT-549 cells (E) determined by nuclear/cytoplasm fractionation assay. (F-G) Representative images and histogram analysis of cell viability after Uc003xsl.1 depletion in MDA-MB-231-P3 (F) and overexpression in BT-549 (G) by EdU assays. Error bars represent standard deviations of three independent experiments. **$p < 0.01$, ***$p < 0.001$.
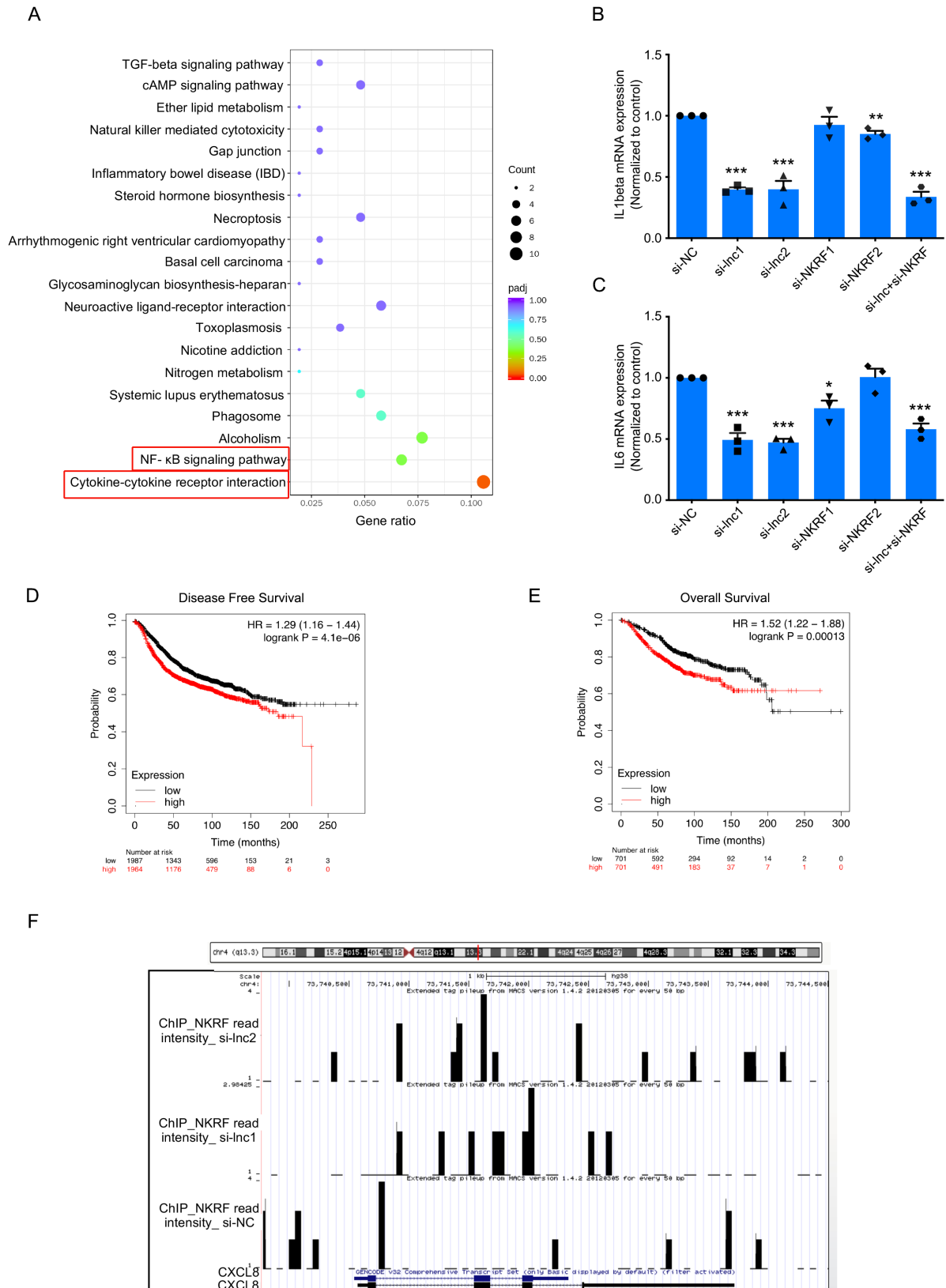
# Supplementary Figure S3



Supplementary Fig. S3

19

**Supplementary Figure S3. Uc003xsl.1 interacts with NKRF to promote NF-κB transcriptional activity-mediated TNBC metastasis.** (A) The levels of Uc003xsl.1 in MDA-MB-231-P3 cells and in MDA-MB-231cells treated with PBS (Mock), control-Vector and Uc003xsl.1-Vector were measured by qRT-PCR. (B) The efficiency of Uc003xsl.1 knockdown in MDA-MB-468 cells was verified by qRT-PCR. (C-D) Cell vitality was measured by MTS assays treated with the formulas in (A) and (B). (E-H) Representative images and histogram analysis of migration and invasion assays in cells treated with the formulas in (A) and (B). Scale bars: 100 μm. (I) RNA pulldown of Uc003xsl.1 followed by Western blot for hnRNPR or hnRNPM in MDA-MB-231-P3 cells. (J) RNA pulldown via sequential truncated Uc003xsl.1 fragments identified the region of Uc003xsl.1 binding with NKRF. The nucleotide 1301–1500 fragment contained the binding motif of Uc003xsl.1 with NKRF. (K) RNA pulldown confirmed that the 1301–1500nts fragment of Uc003xsl.1 binds with NKRF. (L) Total NF-κB transcriptional activity was assessed by luciferase assay in MDA-MB-231-P3 cells after transfection of control siRNA, Uc003xsl.1 siRNA, NKRF siRNA, or both Uc003xsl.1 siRNA and NKRF siRNA. (M) Western blotting was performed to assess phosphorylated P65 expression in MDA-MB-231-P3 cells after transfection of control siRNA, Uc003xsl.1 siRNA, NKRF siRNA, or both of Uc003xsl.1 siRNA and NKRF siRNA. Error bars represent standard deviations of three independent experiments. **$p < 0.01$, ***$p < 0.001$.

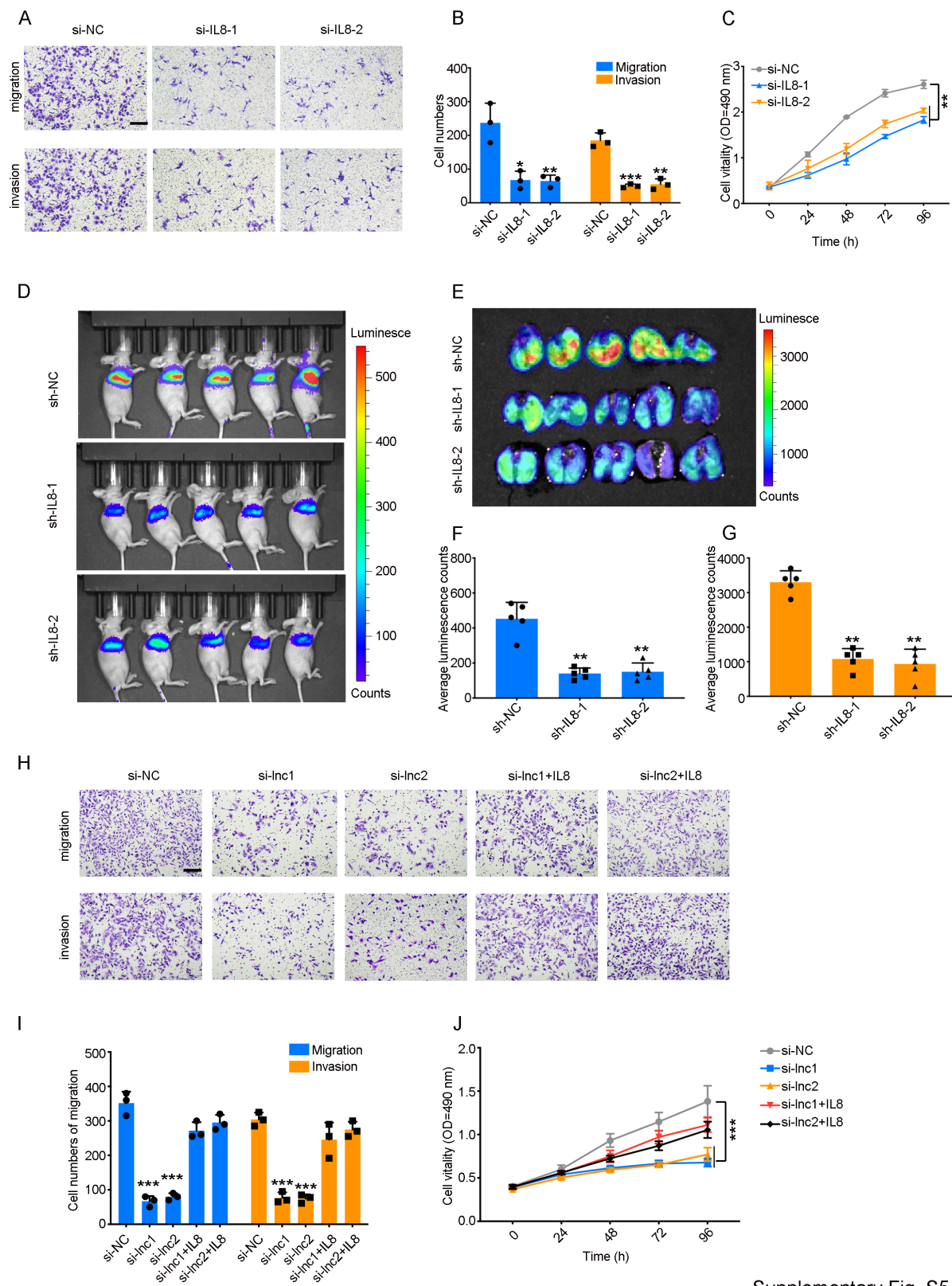# Supplementary Figure S4

A



B



C



D



E



F



Supplementary Fig. S4

**Supplementary Figure S4. ChIP-seq and RNA-seq identify *IL8* as a target gene of the Uc003xsl.1/NKRF complex.** (A) The KEGG analysis based on the altered enrichment of ChIP-seq and RNA-seq upon Uc003xsl.1 silencing. The KEGG focused on signaling pathways and biological processes and was summarized due to the enrichment gene ratio and p values. (B-C) mRNA expression levels of the candidate target gene of *IL1β* (B) and *IL6* (C) were verified by qRT-PCR in MDA-MB-231-P3 cells after transfection of control siRNA, Uc003xsl.1 siRNA, NKRF siRNA, or both of Uc003xsl.1 siRNA and NKRF siRNA. (D-E) TCGA data displayed that patients with high levels of *CXCL8* expression showed reduced DFS (D) and OS (E) than those with low levels of *CXCL8*. (F) Representative enrichment peaks of NKRF in *CXCL8* promoter identified by ChIP-seq in MDA-MB-231-P3 cells after transfection of control siRNA or Uc003xsl.1 siRNA. Error bars represent standard deviations of three independent experiments. *$p < 0.05$, **$p < 0.01$, ***$p < 0.001$.
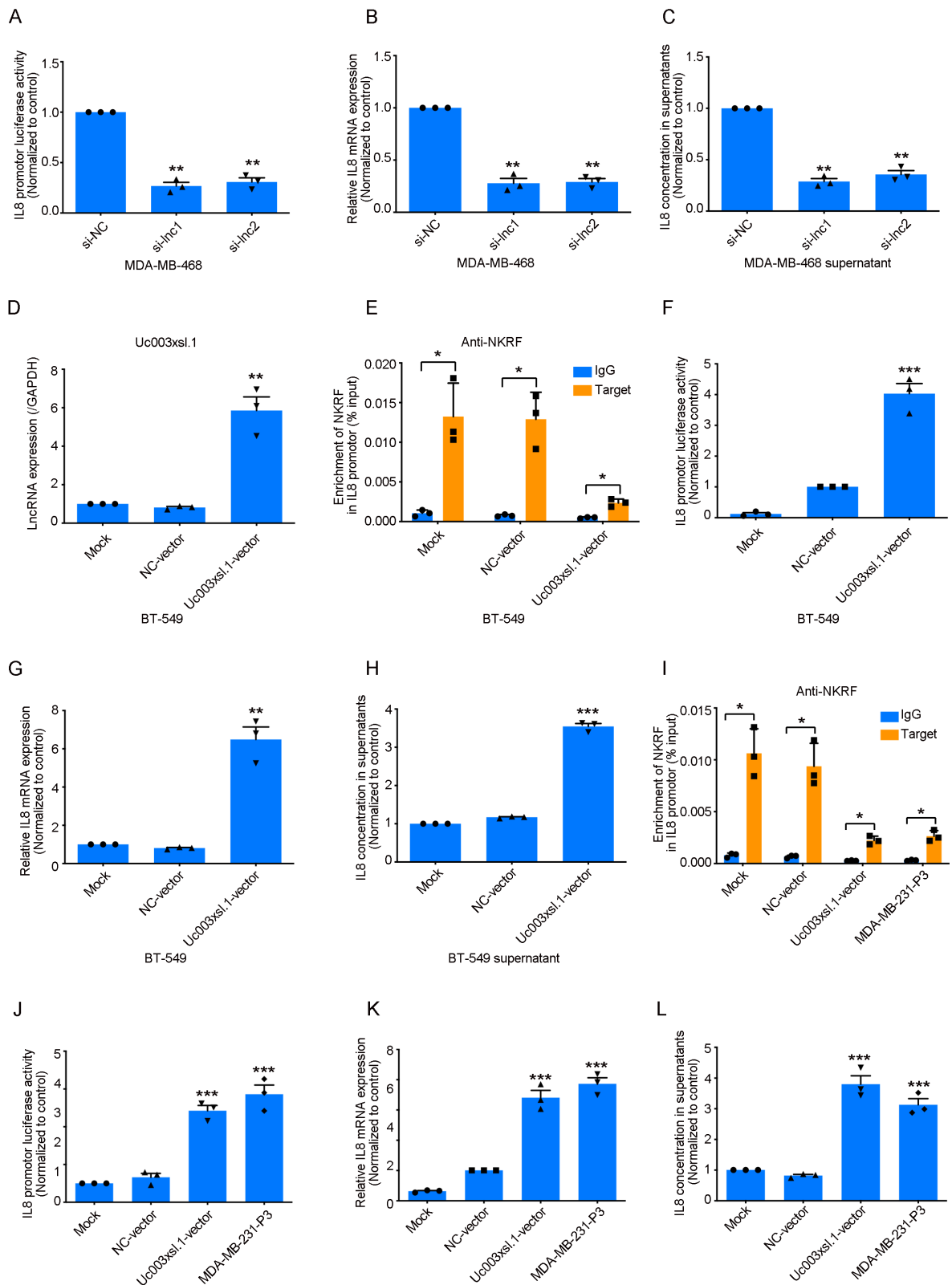
# Supplementary Figure S5

Supplementary Fig. S5

**Supplementary Figure S5. Uc003xsl.1 promotes TNBC metastasis by IL8.** (A–B) Representative images and histogram analysis of transwell assays after IL8 knockdown in MDA-MB-231-P3 cells. Scale bars: 100 μm. (C) Cell viability after IL8 knockdown in MDA-MB-231-P3 cells was assessed by MTS assays. (D-E) Representative bioluminescence images of lung colonization after injection of Luc-MDA-MB-231-P3 cells with sh-NC, sh-IL8-1, and sh-IL8-2 into tail veins (n = 5). Scale bars: 100 μm. (F–G) Histogram analysis for luminescence in Luc-MDA-MB-231-P3 metastatic tumor-bearing nude mice (F) and collected lungs (G). (H-J) Representative images (H), histogram analysis (I) of migration and invasion assays, and MTS assays (J) revealed that treating Uc003xsl.1-silencing MDA-MB-231-P3 cells with 3 ng/mL IL8 partially reversed the effects of cell proliferation, migration and invasion. Scale bars: 100 μm. Error bars represent standard deviations of three independent experiments. **$p < 0.01$, ***$p < 0.001$.
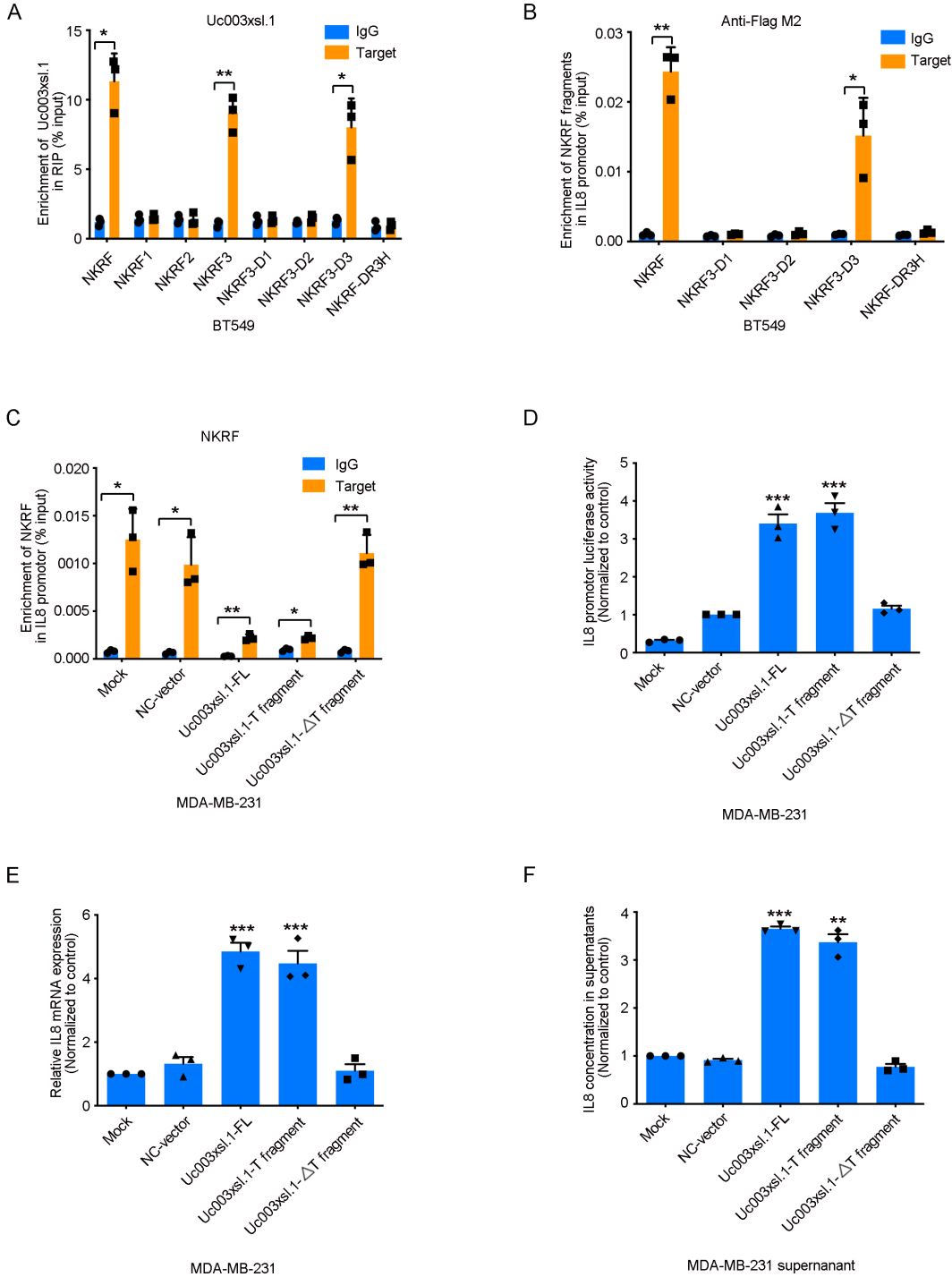
# Supplementary Figure S6



Supplementary Fig. S6

**Supplementary Figure S6. Uc003xsl.1 serves as a molecular decoy between NKRF and**

***IL8.*** (A-C) *IL8* transcriptional activities, mRNA expression levels, and concentrations in supernatants were respectively assessed by luciferase assay (A), qRT-PCR (B), and ELISA (C) in MDA-MB-468 cells treated with si-NC, si-lnc1 and si-lnc2. (D) The expression of Uc003xsl.1 in BT-549 cells treated with PBS (Mock), NC-vector, and Uc003xsl.1-vector. (E) ChIP-PCR analyzed NKRF enrichments in *IL8* promoter in BT-549 cells treated with the formulas in (D). (F-H) *IL8* transcriptional activities, mRNA expression levels, and concentrations in supernatants were respectively assessed by luciferase assay (F), qRT-PCR (G), and ELISA assay (H) in BT-549 cells treated with the formulas in (D). (I) ChIP-PCR analyzed NKRF enrichments in *IL8* promoter in MDA-MB-231-P3 and in MDA-MB-231 cells treated with PBS (Mock), control-Vector and Uc003xsl.1-Vector. (J-L) *IL8* transcriptional activities, mRNA expression levels, and concentrations in supernatants were respectively assessed by luciferase assay (J), qRT-PCR (K), and ELISA (L) in MDA-MB-231-P3 cells and MDA-MB-231 cells treated with formulas in (I). Error bars represent standard deviations of three independent experiments. *$p < 0.05$, **$p < 0.01$, ***$p < 0.001$.

# Supplementary Figure S7

**Supplementary Figure S7. The 1301–1500nts fragment of Uc003xsl.1 mimics the action of a full-length lncRNA.** (A) RIP analysis identified that the NKRF3-D3 fragment specifically binds to Uc003xsl.1 in BT-549 cells. (B) ChIP-PCR analysis revealed that the NKRF3-D3 fragment binds to *IL8* promoter but not the NKRF-DR3H in BT-549 cells. (C) The ChIP-PCR was performed to analyze NKRF enrichments in *IL8* promoter in MDA-MB-231 cells treated with PBS (Mock), NC-vector, Uc003xsl.1-vector, Uc003xsl.1-T-fragment (1301–1500nts) and the mutant deleted 1301–1500nts fragment (Uc003xsl.1- △ T). (D–F) *IL8* transcriptional activities, mRNA expression levels, and concentrations in supernatants were respectively assessed by luciferase assay (D), qRT-PCR (E), and ELISA (F) in MDA-MB-231 cells treated with formulas in (C). Error bars represent standard deviations of three independent experiments. *p < 0.05, **p < 0.01, ***p < 0.001.

# Supplementary Figure S8
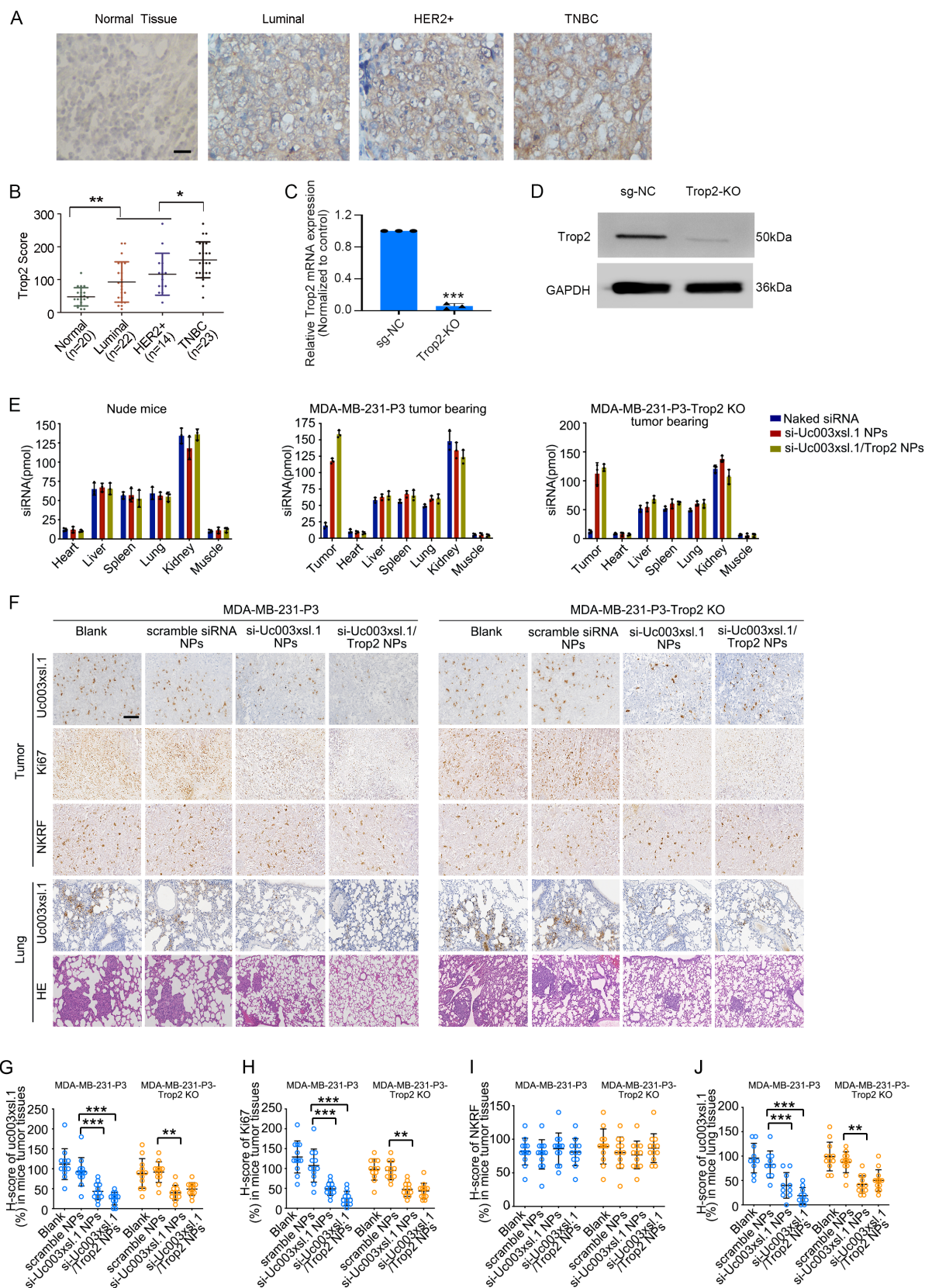


A

Normal Tissue | Luminal | HER2+ | TNBC

B

Trop2 Score

Normal (n=20), Luminal (n=22), HER2+ (n=14), TNBC (n=23)

** *

C

Relative Trop2 mRNA expression (Normalized to control)

sg-NC    Trop2-KO

***

D

sg-NC    Trop2-KO

Trop2        50kDa

GAPDH       36kDa

E

Nude mice

siRNA(pmol)

Heart Liver Spleen Lung Kidney Muscle

MDA-MB-231-P3 tumor bearing

siRNA(pmol)

Tumor Heart Liver Spleen Lung Kidney Muscle

MDA-MB-231-P3-Trop2 KO tumor bearing

siRNA(pmol)

Tumor Heart Liver Spleen Lung Kidney Muscle

■ Naked siRNA
■ si-Uc003xsl.1 NPs
■ si-Uc003xsl.1/Trop2 NPs

F

MDA-MB-231-P3 | MDA-MB-231-P3-Trop2 KO

Blank | scramble siRNA NPs | si-Uc003xsl.1 NPs | si-Uc003xsl.1/Trop2 NPs | Blank | scramble siRNA NPs | si-Uc003xsl.1 NPs | si-Uc003xsl.1/Trop2 NPs

Tumor: Uc003xsl.1, Ki67, NKRF

Lung: Uc003xsl.1, HE

G

H-score of uc003xsl.1 (%) in mice tumor tissues

MDA-MB-231-P3    MDA-MB-231-P3-Trop2 KO

Blank, scramble NPs, si-Uc003xsl.1 NPs, si-Uc003xsl.1/Trop2 NPs

*** *** **

H

H-score of Ki67 (%) in mice tumor tissues

MDA-MB-231-P3    MDA-MB-231-P3-Trop2 KO

Blank, sramble NPs, si-Uc003xsl.1 NPs, si-Uc003xsl.1/Trop2 NPs

*** *** **

I

H-score of NKRF (%) in mice tumor tissues

MDA-MB-231-P3    MDA-MB-231-P3-Trop2 KO

Blank, scramble NPs, si-Uc003xsl.1 NPs, si-Uc003xsl.1/Trop2 NPs

J

H-score of uc003xsl.1 (%) in mice lung tissues

MDA-MB-231-P3    MDA-MB-231-P3-Trop2 KO

Blank, scramble NPs, si-Uc003xsl.1 NPs, si-Uc003xsl.1/Trop2 NPs

*** *** **

Supplementary Fig. S8

29

**Supplementary Figure S8. Si-Uc003xsl.1/Trop2 NPs exerted a significant antitumor effect in vivo.** (A-B) IHC analysis for Trop2 expression in different subtypes of breast cancer tissues. Trop2 was highly expressed in TNBC tissues. Scale bars: 50 μm. (C-D) The Trop2-knockout efficiency was verified in MDA-MB-231-P3-Trop2 KO cells by qRT-PCR (C) and Western blotting (D). (E) Biodistribution of Cy5-siUc003xsl.1 quantified from tumors, and the main organs in nude mice, tumor-bearing nude mice, and Trop2 KO tumor-bearing nude mice at 24h post-injection of the naked siRNA, si-Uc003xsl.1 NPs and si-Uc003xsl.1/Trop2 NPs. (F) Representative images of Uc003xsl.1 expression determined by ISH, Ki67 and NKRF expression determined by IHC, and H&E staining in mice tumor sections or lung sections collected at the endpoint. Scale bars: 100 μm. (G–J) Quantification of Uc003xsl.1 levels in mice tumor sections (G) or lung sections (J) determined by ISH, and Ki67 (H) and NKRF (I) levels in mice tumor sections assessed by IHC collected at the endpoint (Day 26). Error bars represent standard deviations of three independent experiments. *$p < 0.05$, **$p < 0.01$, ***$p < 0.001$.

**Supplementary Figure S9**

A
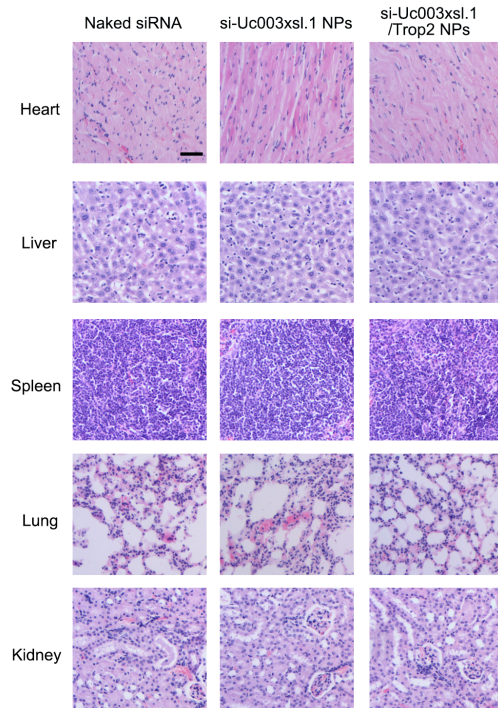


B
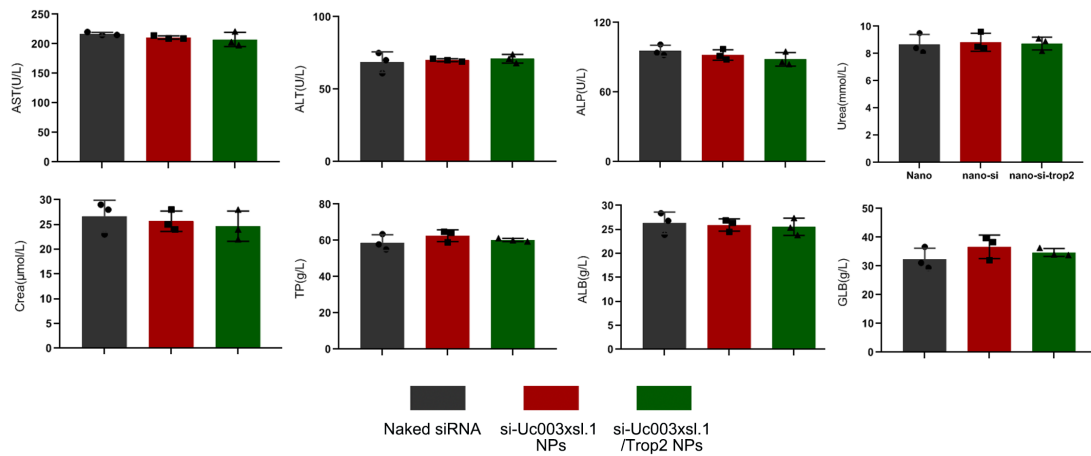
**Supplementary Figure S9. The administration of NPs shows neglectable in vivo side effects.** (A) The H&E staining of major organs of healthy mice (each group, n = 3). No toxicity was detected in tissues from major organs. Scale bars: 100 μm. (B) Hematological parameters, including aspartate aminotransferase, alanine aminotransferase, albumin, alkaline phosphatase, creatinine, and total protein were presented in the normal range after treatment with different types of NPs. Error bars represent standard deviations of three independent experiments.